Research Article

Introducing an optimal pressure ratio for aircraft design and investigating the effect of nozzle efficiency on the jet engine's performance

Hadi SIYAHI[1],* , **Mehdi SIYAHI[1]** , **Mohsen FALLAH[2]** , **Zahra MOHAMMADI[2]**

[1]Aeronautical Engineering Department, Istanbul Technical University, Turkey
[2]Mechanical Engineering Department, Azarbaijan Shahid Madani University, Tabriz, Iran

ABSTRACT

The aviation sector contributes substantially to global transportation energy use, underscoring the critical need for improving energy efficiency in propulsion systems. Conventional energy-based evaluations can sometimes yield misleading results; therefore, exergy-based analysis provides a more realistic understanding of how energy is utilized and degraded within such systems. In this study, a jet engine is analyzed using exergy efficiency as a principal criterion, with specific attention to the effects of compressor pressure ratio and flight altitude. The investigation identifies an optimal operating point that corresponds to the most effective pressure ratio, which also governs engine sizing. The point where the thrust and exergy efficiency curves intersect is proposed as the optimal design condition. Moreover, the role of nozzle efficiency is examined under a range of flight scenarios. The results indicate that at the optimal design points, specific fuel consumption can be reduced by as much as 22.27% at sea level and 13.43% at cruise altitude when compared to maximum thrust conditions. These design points feature lower compressor pressure ratios than those at maximum exergy efficiency, thus improving practical feasibility for real-world applications. Enhancing nozzle efficiency further improves overall engine performance. For instance, at cruise altitude, increasing flight velocity from 100 to 200 m/s and raising nozzle efficiency from 60% to 100% increases thrust by approximately 33–39% and exergy efficiency by 68–71%. At sea level, these improvements reach up to 41% and 73%, respectively. The findings offer valuable insights into achieving concurrent optimization of thrust and exergy efficiency, providing a practical framework for future propulsion and advanced energy system designs.

Cite this article as: Siyahi H, Siyahi M, Fallah M, Mohammadi Z. Introducing an optimal pressure ratio for aircraft design and investigating the effect of nozzle efficiency on the jet engine's performance. J Ther Eng 2026;12(1):1–10.

*Corresponding author.
*E-mail address: siyahi16@itu.edu.tr

INTRODUCTION

The design of efficient aircraft engines is a cornerstone of modern aeronautical engineering, with compressor pressure ratio (CPR) playing a pivotal role in achieving optimal engine performance. A well-designed CPR significantly influences thermodynamic performance, fuel efficiency, and overall thrust generation. Traditional approaches to determine the optimal CPR primarily focus on thermodynamic cycles, such as the Brayton cycle, considering parameters like thermal efficiency and specific fuel consumption [1–3]. However, a growing body of literature suggests that an exergetic approach, which evaluates energy quality and irreversibilities, offers a more comprehensive understanding of engine performance [4–13].

Exergy analysis, unlike conventional energy analysis, accounts for the degradation of useful energy and provides a systematic method to assess efficiency improvements. Researchers have explored exergetic methodologies to optimize energy systems [14]. Others applied these principles to aircraft engines, demonstrating the effectiveness of exergy-based optimization in aviation [2,15–17].

Despite these advancements, the nozzle's contribution to jet engine performance, particularly in relation to exergetic efficiency, remains underexplored. Former studies have highlighted the critical role of nozzle efficiency in thrust generation. These works have shown that nozzle losses can significantly degrade overall engine performance, particularly in high-performance engines. However, there is limited integration of nozzle efficiency considerations into a holistic exergetic optimization framework.

Moreover, a significant gap in the literature lies in the simultaneous evaluation of thrust, exergy efficiency, and CPR optimization. While individual studies have addressed thrust or exergy efficiency independently, the coupling of these metrics for determining optimal CPR has received scant attention. This integrated approach is vital for developing design guidelines that balance thrust generation and exergy efficiency, thereby enhancing the performance and sustainability of jet engines.

This paper seeks to address this gap by developing a comprehensive framework that integrates thrust and exergy efficiency into optimizing CPR for aircraft engine design. The study highlights the interplay between CPR, nozzle efficiency, and exergetic performance, providing insights into achieving higher thermodynamic and operational efficiency. By bridging the gap between traditional thermodynamic metrics and exergy-based performance analysis, this work aims to establish a novel methodology for designing high-efficiency jet engines.

GOVERNING EQUATIONS

Energy can be explained as the summation of exergy and anergy [18–22]:

$$Energy = Exergy + Anergy \qquad (1)$$

where exergy and anergy are maximum accessible work and non-accessible work, respectively.

The specific energy can be written as [18–22]:

$$e = h + \frac{V^2}{2} + gz \qquad (2)$$

where h, $V^2/2$ and gz are specific enthalpy, kinetic and potential energy terms, respectively.

In the absence of the effects of nuclear, magnetic, electric, and surface tension fields, the specific exergy can be written as summation of physical, chemical, kinetic, potential, heat and work exergy terms [18–22]:

$$ex = ex_{ph} + ex_{ch} + ex_k + ex_p + ex_q + ex_w \qquad (3)$$

where $ex_{ph} = (h-h_0) - T_0(s-s_0)$, $ex_{ch} = (\Delta h_{formation} - T_0 \Delta s_{formation}) + T_0 R \Sigma(y^i ln y^i / y^i_0)$, $ex_k = v^2/2$, and $ex_p = gz$. Temperatures in these equations are in Kelvin. The exergy values of heat and work are $ex_q = \left(1 - \frac{T_0}{T}\right) q$ and $ex_w = w$, respectively, where temperatures in the ex_q equation are in Kelvin.
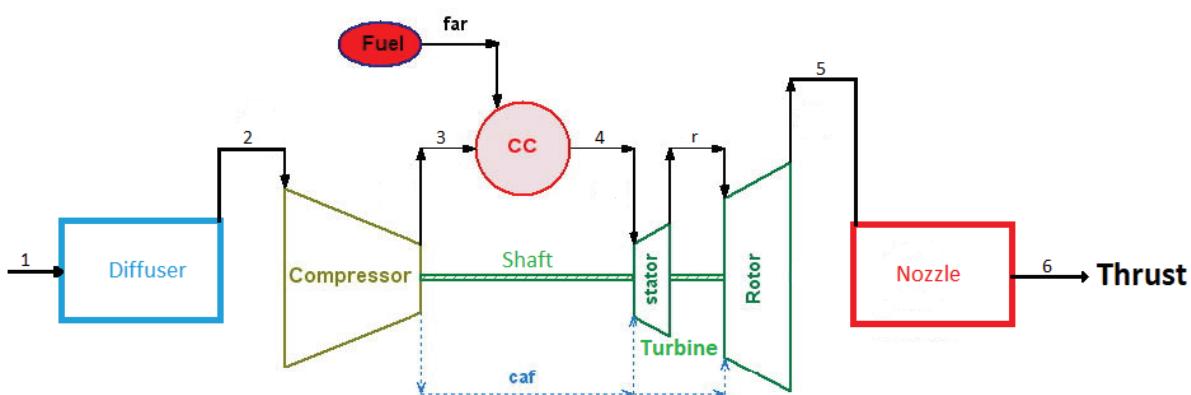

Figure 1. Schematic of a jet engine.

Noticing that 1, 2, 3, 4, 5 and 6 states in Figure 1 respectively introduce the diffuser inlet, compressor inlet (diffuser outlet), combustion chamber inlet (compressor outlet), turbine inlet (combustion chamber outlet), nozzle inlet (turbine outlet) and exhaust (nozzle outlet), all equations required for the energy-exergy analyses and thermodynamic optimization of jet engine have been summarized in Table 1 [18–29].

RESULTS AND DISCUSSION

Validation

An engineering equation solver (EES) program has been written for an open simple gas turbine cycle with methane (CH4) as a fuel and results have been compared with reference study [30].

The related equations have been written for the compressor, combustion chamber and turbine, and results have

Table 1. Thermodynamics equations for energy-exergy analyses [18–29]

Components	Related equations
Diffuser	$\dot{m}_2 = \dot{m}_1$ $\dot{m}_2\left(h_2 + \dfrac{v_2^2}{2}\right) = \dot{m}_1\left(h_1 + \dfrac{v_1^2}{2}\right), v_1 = v_{inlet}, v_2 = 0$ $\eta_{I,diff,isen} = \dfrac{\left(\dot{m}_2 h_{2,isen} - \dot{m}_1 h_1\right)}{\left(\dot{m}_2 h_2 - \dot{m}_1 h_1\right)}, P_2 = P_{2,isen}$ $\dot{Ex}_{D,diff} = \dot{m}_1 ex_1 - \dot{m}_2 ex_2$ $\eta_{II,diff} = \dfrac{\dot{m}_2 ex_2}{\dot{m}_1 ex_1}$
Compressor	$\dot{m}_3 = (1 - caf)\dot{m}_2$ $\dot{W}_{comp} = \dot{m}_2(e_3 - e_2)$ $\eta_{I,comp,poly} = \dfrac{\bar{R}T\dfrac{dp}{p}}{\bar{C}_{p,air}dT}$ $\dot{Ex}_{D,comp} = \dot{W}_{comp} + \dot{m}_2(ex_2 - ex_3)$ $\eta_{II,comp} = \dfrac{\left(\dot{W}_{comp} - \dot{Ex}_{D,comp}\right)}{\dot{W}_{comp}}$
Cooling air fraction	$T_r = 0.8451(TIT) + 136.2, T_r \text{ and } TIT \text{ are in } °C$ $caf = \dfrac{2(1 + far)(e_4 - e_r)}{(2e_4 - e_3 - e_r)}$ $\dot{m}_{caf} = (caf)\dot{m}_1$
Combustion chamber	$\dot{m}_4 = \dot{m}_3 + \dot{m}_{fuel}, \dot{m}_{fuel} = (far)\dot{m}_1$ $\int_{298.15}^{T_f} \bar{C}_{p,C_nH_m}dT + \lambda\left(n + \dfrac{m}{4}\right)\left[\int_{298.15}^{T_3} \bar{C}_{p,O_2}dT + 3.76\int_{298.15}^{T_3} \bar{C}_{p,N_2}dT\right.$ $\left. + 4.76\bar{\omega}_1\int_{298.15}^{TIT} \bar{C}_{p,H_2O}dT\right] = n\int_{298.15}^{TIT} \bar{C}_{p,CO_2}dT + (\lambda - 1)\left(n + \dfrac{m}{4}\right)\int_{298.15}^{TIT} \bar{C}_{p,O_2}dT$ $+ 3.76\lambda\left(n + \dfrac{m}{4}\right)\int_{298.15}^{TIT} \bar{C}_{p,N_2}dT + \left[\lambda\left(n + \dfrac{m}{4}\right)4.76\bar{\omega}_1 + \dfrac{m}{2}\right]\int_{298.15}^{TIT} \bar{C}_{p,H_2O}dT$ $far = \dfrac{M_{C_nH_m}}{\lambda\left(n + \dfrac{m}{4}\right)4.76(1 + \bar{\omega}_1)M_{air}\eta_{I,cc}}(1 - caf)$ $\dot{m}_3 e_3 + \dot{m}_{fuel}e_{fuel} = \dot{m}_4 e_4$ $\eta_{I,cc} = \dfrac{far_{ideal}}{far}$ $\dot{Ex}_{D,cc} = \dot{m}_3 ex_3 + \dot{m}_{fuel}ex_{fuel} - \dot{m}_4 ex_4$ $\eta_{II,cc} = \dfrac{\dot{m}_4 ex_4}{\dot{m}_3 ex_3 + \dot{m}_{fuel}ex_{fuel}}$

Table 1. Thermodynamics equations for energy-exergy analyses [18–29] (continued)

Components	Related equations
Turbine	$\dot{m}_5 = (1 + far)\dot{m}_1$ $\dot{W}_{turb} = \dot{W}_{comp}$ $\dot{W}_{turb} = \dot{m}_{caf}e_3 + \dot{m}_4 e_4 - \dot{m}_5 e_5$ $\eta_{I,turb,poly} = \dfrac{\bar{C}_{p,g}\,dT}{\bar{R}T\dfrac{dp}{p}}$ $\dot{Ex}_{D,turb} = \dot{m}_{caf}ex_3 + \dot{m}_4 ex_4 - \dot{m}_5 ex_5 - \dot{W}_{turb}$ $\eta_{II,turb} = \dfrac{\dot{W}_{turb}}{\left(\dot{W}_{turb} + \dot{Ex}_{D,turb}\right)}$
Nozzle	$\dot{m}_6 = \dot{m}_5$ $\dot{m}_6\left(h_6 + \dfrac{v_6^2}{2}\right) = \dot{m}_5\left(h_5 + \dfrac{v_5^2}{2}\right), v_5 = 0, P_6 = P_0$ $\eta_{I,nozz,isen} = \dfrac{(\dot{m}_6 h_6 - \dot{m}_5 h_5)}{\left(\dot{m}_6 h_{6,,isen} - \dot{m}_5 h_5\right)}, P_6 = P_{6,isen}$ $\dot{Ex}_{D,nozz} = \dot{m}_5 ex_5 - \dot{m}_6 ex_6$ $\eta_{II,nozz} = \dfrac{\dot{m}_6 ex_6}{\dot{m}_5 ex_5}$
Cycle	$\dot{Thrust} = \dot{m}_6(V_6 - V_1)$ $\eta_{I,cycle} = \dfrac{\dot{m}_6\left(\dfrac{v_6^2}{2} - \dfrac{v_1^2}{2}\right)}{\dot{m}_{fuel}LHV}$ $\dot{Ex}_{D,cycle} = \dot{Ex}_{D,diff} + \dot{Ex}_{D,comp} + \dot{Ex}_{D,cc} + \dot{Ex}_{D,turb} + \dot{Ex}_{D,nozz}$ $\eta_{II,cycle} = \dfrac{\dot{m}_6\left(\dfrac{v_6^2}{2} - \dfrac{v_1^2}{2}\right)}{\dot{m}_1 ex_1 + \dot{m}_{fuel}ex_{fuel}}$

been revealed through the calculations of compressor outlet temperature (COT), turbine inlet temperature (TIT), and turbine outlet temperature (TOT) via EES program. Analysis indicates that the data differ by no more than 3.5%, which falls within an acceptable margin for this type of parametric evaluation (Table 2).

Table 2. The Validation of EES Program's Data for Simple Gas Turbine Cycle vs. Reference [30]

Variables	Reference	Present study	Deviation
T_0	15 °C	15 °C	0.0%
P_0	101 kPa	101 kPa	0.0%
RH_0	60%	60%	0.0%
$r_{p,comp}$	20	20	0.0%
$\eta_{I,comp,poly}$	92%	92%	0.0%
COT	449.6 °C	438.6 °C	2.4%
$\eta_{I,cc}$	100%	100%	0.0%
TIT	1331.3 °C	1330 °C	0.1%
$\eta_{I,turb,poly}$	86%	89%	3.5%
TOT	620 °C	617.1 °C	0.5%

Jet engine

The jet engine performance was analyzed under steady-state steady-flow (SSSF) conditions using a two-stage turbine with blade cooling [29]. Dodecane ($C_{12}H_{26}$) was selected as the fuel, and the energy efficiencies of the diffuser, compressor, combustion chamber, turbine, and nozzle were assumed to be 90%, 95%, 100%, 92%, and 90%, respectively. The combustion process was modeled as an isobaric reaction with a constant turbine inlet temperature of 1200°C across all cases. Parametric studies were conducted at sea level (T_0 = 25°C, P_0 = 101.325 kPa, RH_0 = 30%) and cruise altitude (T_0 = −56.5°C, P_0 = 22.6 kPa, RH_0 = 0%). Key performance indicators, including thrust, exergy destruction, energy efficiency, and exergy efficiency, were evaluated across various compressor pressure ratios. It is important to note that all results are expressed on a mass basis (per 1 kg of inlet air) rather than on a volumetric basis (per 1 m³ of inlet air).

The results indicate that maximum thrust is achieved within a low CPR range of 15 to 25 across all scenarios. At cruise conditions, higher thrust levels are observed, though less thrust is required as flight speed increases to maintain

steady flight. Exergy destruction shows a consistent decline with increasing CPR, as illustrated in Figure 2.

Energy and exergy efficiencies exhibit distinct patterns. At sea level, these efficiencies peak at CPR values of 50 to 60, whereas at cruise altitude, optimal efficiencies are reached at CPR values exceeding 100 (Figure 3).

Additionally, the cooling air fraction (caf) and fuel-air ratio (far) respond to changes in CPR and altitude. The far increases with altitude due to lower ambient temperatures, which require higher fuel input to sustain TIT, while caf decreases as inlet air cooling capacity improves (Figure 4).
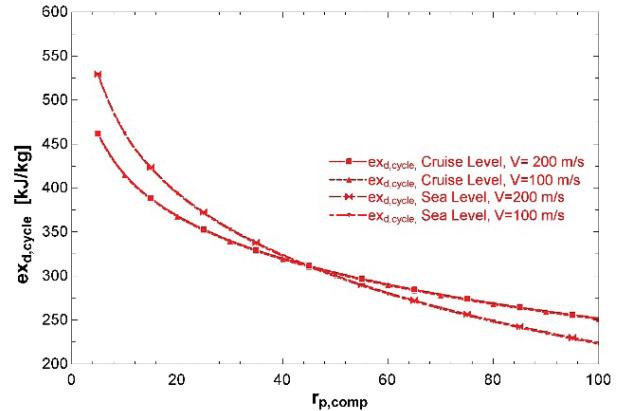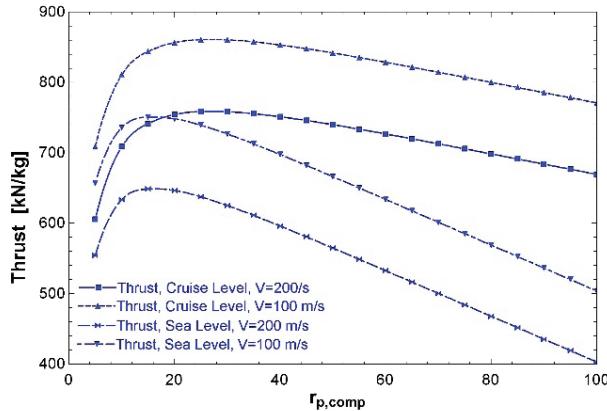

**Figure 2.** Thrust production and exergy destruction of jet engine at different flight scenarios.
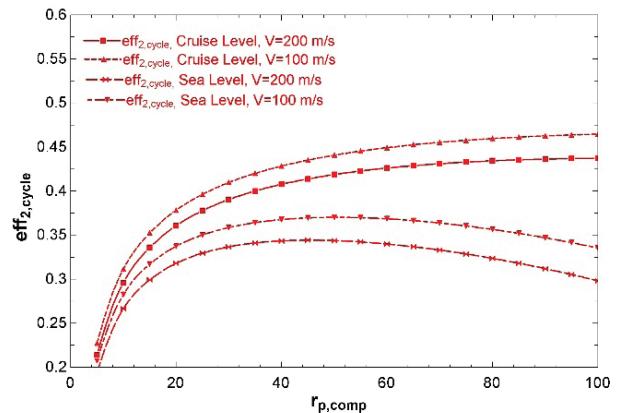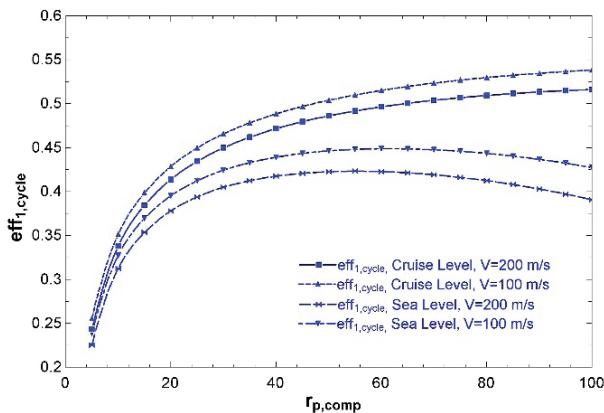
**Figure 3.** Energy and exergy efficiency of jet engine at different flight scenarios.
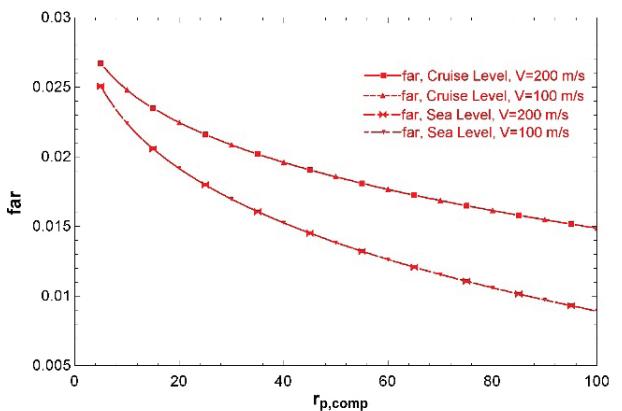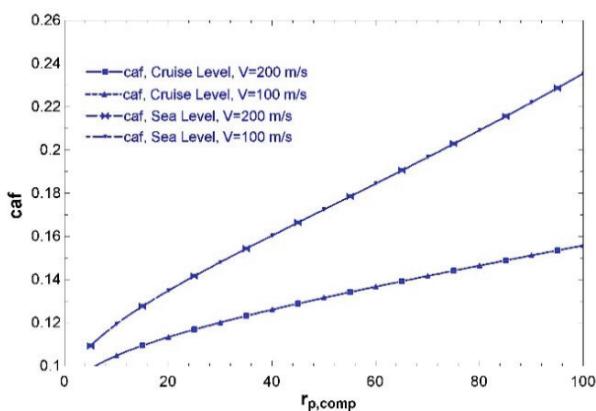
Figure 4. Cooling air fraction and fuel air ratio of jet engine at different flight scenarios.
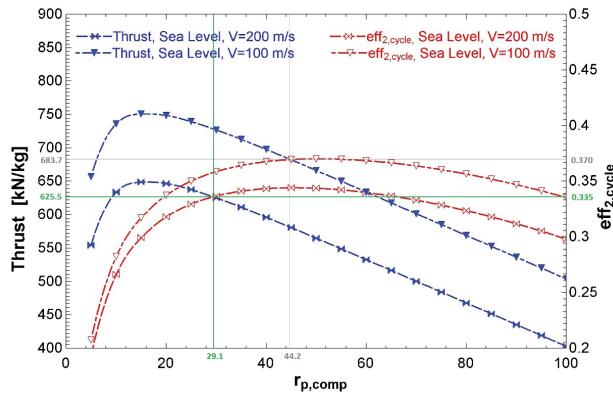
Figure 5. Max simultaneous thrust- exergy efficiency as an operating design point at sea level
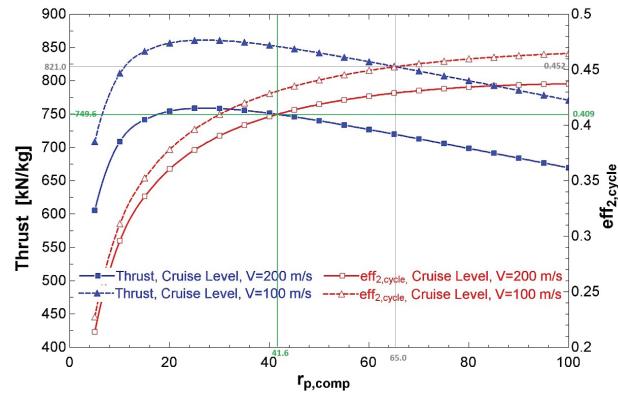

Figure 6. Max simultaneous thrust- exergy efficiency as an operating design point at cruise level

Table 3. Design point's pressure ratios for different flight scenarios

Flight Scenario	$r_{p,comp}$
Sea level, V=100 m/s	44.2
Sea level, V=200 m/s	29.1
Cruise level, V=100 m/s	65.0
Cruise level, V=200 m/s	41.6

The intersection of thrust and exergy efficiency curves, identified as the optimal design point, marks the CPR where simultaneous maximization of these parameters occurs. Figures 5 and 6 highlight this phenomenon, with the corresponding CPR values summarized in Table 3. These optimal CPR values exhibit a direct correlation with altitude and an inverse correlation with flight speed.

All performance parameters of the jet engine at design points have been plotted in the bar diagram of Figure 7. As can be seen in this diagram, while exergy destruction is increased thrust, energy efficiency, and exergy efficiency of jet engine are decreased with speeding of an aircraft. Moreover, all performance parameters of jet engine are upgraded with rising altitude.

As illustrated in Figure 8, the specific fuel consumption (SFC) at the optimal design points decreases by 22.27% to 14.44% at sea flight level and by 13.43% to 5.15% at cruise flight level, compared to the SFC at maximum thrust conditions for velocities of 100 m/s and 200 m/s, respectively. Furthermore, Figures 5 and 6 indicate that the optimal design points exhibit significantly lower compressor pressure ratios compared to the points with maximum exergy efficiency. The reduced SFC and pressure ratio at the optimal points, alongside simultaneous maximization of thrust
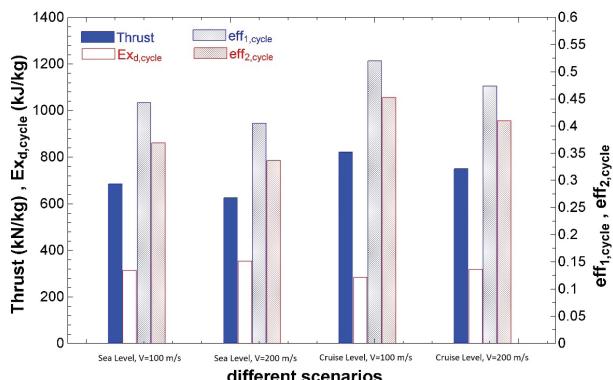

Figure 7. Performance parameters of jet engine at design point for different flight scenarios.
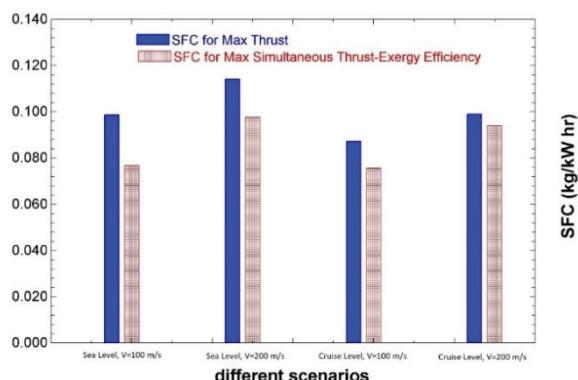

Figure 8. Comparison of specific fuel consumption at max thrust and optimal design point for different flight scenarios.

and exergy efficiency, makes these points highly favorable from a practical design perspective.

Eventually, the effect of nozzle energy efficiency is investigated on the jet engine's performance, revealing changes of the most critical design parameters of thrust and exergy efficiency at previously mentioned operating design conditions.

As disclose in Figure 9, at sea level, by increasing the efficiency of nozzle from 60 to 100% the thrust is increased from 540.7 to 727.4 kN/kg , and the exergy efficiency of engine boosts from 24.4% to 41.1%, for the speed of V = 100 m/s. These values for the speed of V = 200 m/s are 473.2 to 670.1 kN/kg thrust increase, and 21.7% to 37.7% exergy efficiency boost. At cruise level, for the same nozzle efficiency improvement in Figure 10, the similar values at cruise level are 652.3 to 871.7 kN/kg and 578.2 to 805.9 kN/kg increase in thrust, with 30.0% to 50.4% and 26.3% to 45.1% boost in exergy efficiency, for the speeds of V = 100 m/s and V = 200 m/s, respectively.

As shown in Table 4, the performance improvement of a jet engine with increasing nozzle efficiency is even greater for sea level flight altitude at the optimal design points.

Jet engine performance is significantly influenced by the pressure ratio and nozzle efficiency, as they determine the thrust and efficiency of the engine. Meanwhile, there are the limitations of each. Higher pressure ratios lead to higher temperatures in the combustion chamber and turbine. These temperatures can exceed material limits, requiring advanced cooling techniques or high-temperature materials. As the pressure ratio increases, the compressor stages require higher efficiency. Beyond a certain point, increasing pressure ratio results in diminishing returns due to inefficiencies, such as mechanical losses and flow separation. High pressure ratios can increase the risk of compressor stall or surge, especially at off-design conditions, reducing operational reliability. Higher pressure

Table 4. Design point's thrust and overall exergy efficiency improvements by increasing nozzle energy efficiency from 60% to 100% for different flight scenarios

Flight Scenario	Improvement	
	Thrust	$\eta_{II,cycle}$
Sea level, V=100 m/s	34.5%	68.4%
Sea level, V=200 m/s	41.6%	73.7%
Cruise level, V=100 m/s	33.6%	68.0%
Cruise level, V=200 m/s	39.3%	71.4%

ratios demand more work from the turbine to drive the compressor, which can limit the available for thrust generation. Increasing the pressure ratio typically requires more compressor stages, which adds weight and mechanical complexity to the engine. Very high-pressure ratios might not match the ideal cycle conditions for specific flight regimes, such as low-speed or high-altitude operations. On the other hand, low nozzle efficiency results in incomplete conversion of thermal and pressure energy into kinetic energy, reducing thrust output. At off-design conditions, such as low-speed or high-altitude operation, flow separation within the nozzle can reduce efficiency and stability. In supersonic nozzles, imperfect expansion due to mismatched atmospheric pressure can lead to shock waves, causing energy losses and efficiency reduction. At varying altitudes, the nozzle may be under-expanded (not fully converting pressure) or over-expanded (causing shocks and flow separation), limiting efficiency. If the nozzle material is not adequately insulated, heat losses can occur, slightly reducing the energy available for thrust. Designing a nozzle optimized for multiple flight regimes (subsonic, transonic, supersonic) is challenging. Fixed geometry nozzles may perform sub-optimally in some conditions, while variable
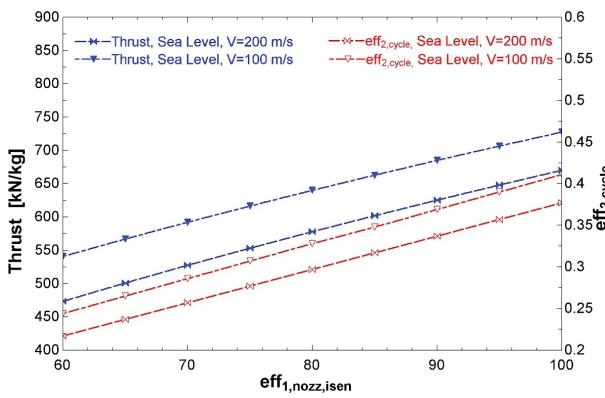

Figure 9. Improvement of jet engine performance operating in optimal design condition by increasing nozzle efficiency at sea level
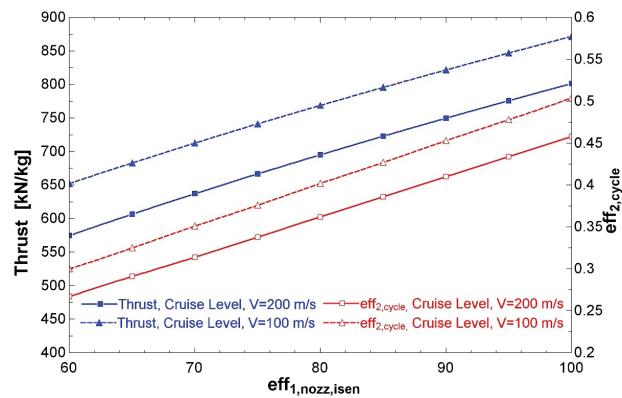

Figure 10. Improvement of jet engine performance operating in optimal design condition by increasing nozzle efficiency at cruise level

geometry nozzles add weight and mechanical complexity. Considering the combined impact on performance, a proper high-pressure ratio and efficient nozzle are essential for maximizing thrust and minimizing SFC. Limitations in either reduce overall engine performance. Higher pressure ratios improve efficiency, but this is only beneficial if the nozzle effectively converts the energy into thrust. By balancing these limitations, the design of jet engines should meet the specific performance requirements for different aircraft types and missions.

The analysis of the present research underscores the critical role of optimal CPR and nozzle efficiency in enhancing jet engine performance at different flight scenarios. Achieving maximum simultaneous thrust and exergy efficiency at practical design points provides significant operational benefits, including reduced SFC and improved sustainability.

CONCLUSION

This study provides a comprehensive investigation into the optimization of jet engine performance using an energy-exergy analysis framework. By introducing the concept of the optimal design point as the optimum compressor pressure ratio of the intersection of thrust and exergy efficiency curves, a novel methodology for jet engine design optimization is proposed. This approach considers variations in compressor pressure ratio (CPR), flight altitude, and nozzle efficiency.

The findings demonstrate that the optimal design points significantly enhance the practical viability of engine operation. At sea level, the specific fuel consumption (SFC) at the optimal conditions is reduced by up to 22.27%, while at cruise altitudes, it decreases by 13.43%, compared to maximum thrust conditions. These results emphasize the importance of balancing thrust and exergy efficiency for achieving sustainable and efficient engine designs. Furthermore, the study reveals that the optimal CPR is lower than CPR value at maximum exergy efficiency, making the design both practical and efficient for real-world applications.

A critical aspect of this research is the impact of nozzle efficiency on engine performance. Enhancing nozzle efficiency from 60% to 100% leads to substantial improvements in thrust and exergy efficiency under optimal design conditions. At sea level, thrust increases by up to 41%, while exergy efficiency improves by 73%. Similarly, at cruise altitude, these parameters are enhanced by up to 39% and 71%, respectively. These improvements highlight the vital role of nozzle efficiency in maximizing engine performance and reducing environmental impact.

The study also addresses the limitations of high-pressure ratios and nozzle inefficiencies, including mechanical complexities, material constraints, and off-design performance challenges. By integrating these considerations into the optimization framework, the research offers valuable insights into the design trade-offs required for efficient propulsion systems.

In summary, this research bridges the gap between traditional thermodynamic approaches and exergy-based methodologies, offering a robust framework for the future design and optimization of jet engines. The results provide actionable guidance for achieving higher efficiency, reduced fuel consumption, and improved sustainability in aviation propulsion systems, setting a benchmark for innovative and environmentally conscious aerospace engineering solutions.

NOMENCLATURE

e	Specific energy, kJ / kg
eff	Dimensionless efficiency
ex	Specific exergy, kJ / kg
g	Gravitational acceleration constant, m / s^2
M	Molar mass, kg / kmole
$Mach$	Dimensionless mach number
$\dot{m}$	Mass flow rate, kg / s
P	Pressure, Pa
q	Specific heat rate, kJ / kg
r_p	Dimensionless pressure ratio
s	Specific entropy, kJ / kg
t	Time, s
T	Temperature, °C
V	Velocity, m / s
w	Specific work rate, kJ / kg

Greek symbols

λ	Dimensionless excess air
η	Dimensionless efficiency

Subscripts

1 *or I*	First law or energetic
2 *or II*	Second law or exergetic
0	Ambient condition
cc	Combustion chamber
ch	Chemical
comp	Compressor
D	Destruction
diff	Diffuser
isen	Isentropic
k	Kinetic
nozz	Nozzle
p	Potential
ph	Physical
poly	Polytropic
q	Heat
r	Rotator
turb	Turbine
w	Work

Abbreviations

caf	Cooling air fraction
COT	Compressor outlet temperature

CPR	Compressor pressure ratio
far	Fuel air ratio
RH	Relative humidity
SFC	Specific fuel consumption
SSSF	Steady state steady flow
TIT	Turbine inlet temperature
TOT	Turbine outlet temperature

AUTHORSHIP CONTRIBUTIONS

Authors equally contributed to this work.

DATA AVAILABILITY STATEMENT

The authors confirm that the data that supports the findings of this study are available within the article. Raw data that support the finding of this study are available from the corresponding author, upon reasonable request.

CONFLICT OF INTEREST

The author declared no potential conflicts of interest with respect to the research, authorship, and/or publication of this article.

ETHICS

There are no ethical issues with the publication of this manuscript.

STATEMENT ON THE USE OF ARTIFICIAL INTELLIGENCE

Artificial intelligence was not used in the preparation of the article.

REFERENCES

[1] Durmus S, Akyuz MK. Effect of compression ratio and turbine inlet temperature on turboprop engine performance. IENSC 2020;299–307.

[2] Ekrataleshian A, Pourfayaz F, Ahmadi MH. Thermodynamic and thermoeconomic analyses and energetic and exergetic optimization of a turbojet engine. J Therm Anal Calorim 2021;145:909–923. [CrossRef]

[3] Raji NA, Kuku RO, Openibo AO, Owolabi EA. Influence of compression ratio on the performance characteristics of a spark ignition engine. J Prod Eng 2024;27;5–12. [CrossRef]

[4] Tsatsaronis G. Strengths and limitations of exergy analysis. Thermodynamic optimization of complex energy systems. Springer 1999;93–100. [CrossRef]

[5] Bejan A, Siems DL. The need for exergy analysis and thermodynamic optimization in aircraft development. Exergy, An International Journal 2001;1:14–24. [CrossRef]

[6] Paulus Jr DM, Gaggioli RA. The exergy of lift, and aircraft exergy flow diagrams. ASME International Mechanical Engineering Congress and Exposition 2001;35524:365–9. [CrossRef]

[7] Rosen MA, Etele J. Aerospace systems and exergy analysis: applications and methodology development needs. Int J Exergy 2004;1:411–25. [CrossRef]

[8] Riggins DW, Taylor T, Moorhouse DJ. Methodology for performance analysis of aerospace vehicles using the laws of thermodynamics. J Aircr 2006;43:953–63. [CrossRef]

[9] Dong Z, Li D, Wang Z, Sun M. A review on exergy analysis of aerospace power systems. Acta Astronaut 2018;152:486–95. [CrossRef]

[10] Sohret Y. Exergo-sustainability analysis and ecological function of a simple gas turbine aero-engine. J Therm Eng 2018;4:2083–95. [CrossRef]

[11] Ball O. Performance assessment of a medium-scale turboprop engine designed for unmanned aerial vehicle (UAV) based on exergetic and sustainability metrics. J Therm Eng 2020;6:697–711. [CrossRef]

[12] Reddy PN. Energy and exergy analyses of a two-stage organic rankine cycle with low pressure stage regeneration for IC engine waste heat recovery. J Therm Eng 2021;8:573–86. [CrossRef]

[13] Khan MN. Combined effect of variable parameters on the performance of gas turbine cycles. J Therm Eng 2021;7:1768–83. [CrossRef]

[14] James C, Kim TY, Jane R. A review of exergy based optimization and control. Processes 2020;8:364. [CrossRef]

[15] Rancruel DF, von Spakovsky MR. Decomposition with thermoeconomic isolation applied to the optimal synthesis/design and operation of an advanced tactical aircraft system. Energy 2006;31:3327–41. [CrossRef]

[16] Aygun H. Optimization of energy and exergy parameters for a conceptual after burning turbojet engine. J Therm Eng 2021;9:69–85. [CrossRef]

[17] Aygun H, Kirmizi M, Kilic U, Turan O. Multi-objective optimization of a small turbojet engine energetic performance. Energy 2023;271:126983. [CrossRef]

[18] Borgnakke C, Sonntag RE. Fundamentals of thermodynamics. John Wiley & Sons; 2020.

[19] Annamalai K, Puri IK, Jog MA. Advanced thermodynamics engineering. CRC press; 2011.

[20] Winterbone D, Turan A. Advanced thermodynamics for engineers. Butterworth-Heinemann; 2015.

[21] Bejan A. Advanced engineering thermodynamics. John Wiley & Sons; 2016.

[22] Tabatabaian M, Rajput RK. Advanced thermodynamics: fundamentals, mathematics, applications. De Gruyter. [CrossRef]

[23] Oates GC. Aerothermodynamics of gas turbine and rocket propulsion. Aiaa 1997. [CrossRef]

[24] Mattingly JD. Elements of propulsion: gas turbines and rockets. American Institute of Aeronautics and Astronautics; 2006.

[25] MacIsaac B, Langton R, Belobaba P, Cooper J, Seabridge A. Gas turbine propulsion systems. John Wiley & Sons 2011. [CrossRef]

[26] El-Sayed AF. Fundamentals of aircraft and rocket propulsion. Springer 2016. [CrossRef]

[27] El-Sayed AF. Aircraft propulsion and gas turbine engines. CRC press; 2017.

[28] Siyahi M, Siyahi H, Fallah M, Mohammadi Z. Thermodynamic Optimization and Energy-Exergy Analyses of the Turboshaft Helicopter Engine. Int J Thermodyn 2024:1–11. [CrossRef]

[29] Fallah M, Siyahi H, Ghiasi RA, Mahmoudi SMS, Yari M, Rosen MA. Comparison of different gas turbine cycles and advanced exergy analysis of the most effective. Energy 2016;116:701–15. [CrossRef]

[30] Pathirathna KAB. Gas turbine thermodynamic and performance analysis methods using available catalog data 2013.